

Deassociate the initial temporal phase deviation provided by photoelastic modulator for stroboscopic illumination polarization modulated ellipsometry

Hsiu-Ming Tsai, Chih-Wei Chen, Tsung-Han Tsai, and Yu-Faye Chao

Citation: [Review of Scientific Instruments](#) **82**, 035117 (2011); doi: 10.1063/1.3568745

View online: <http://dx.doi.org/10.1063/1.3568745>

View Table of Contents: <http://scitation.aip.org/content/aip/journal/rsi/82/3?ver=pdfcov>

Published by the [AIP Publishing](#)

Articles you may be interested in

[Spectroscopic ellipsometry study of hydrogenated amorphous silicon carbon alloy films deposited by plasma enhanced chemical vapor deposition](#)

[J. Appl. Phys.](#) **107**, 023502 (2010); 10.1063/1.3277016

[Influence of the implantation profiles of Si + on the dielectric function and optical transitions in silicon nanocrystals](#)

[J. Chem. Phys.](#) **129**, 184701 (2008); 10.1063/1.3009223

[Photoelastic modulated imaging ellipsometry by stroboscopic illumination technique](#)

[Rev. Sci. Instrum.](#) **77**, 023107 (2006); 10.1063/1.2173027

[Structural and optical investigation of plasma deposited silicon carbon alloys: Insights on Si-C bond configuration using spectroscopic ellipsometry](#)

[J. Appl. Phys.](#) **97**, 103504 (2005); 10.1063/1.1899758

[Five layer stack of nitride, oxide, and amorphous silicon on glass, analyzed with spectroscopic ellipsometry](#)

[J. Vac. Sci. Technol. A](#) **15**, 992 (1997); 10.1116/1.580793

JANIS

**Does your research require low temperatures? Contact Janis today.
Our engineers will assist you in choosing the best system for your application.**



10 mK to 800 K
Cryocoolers
Dilution Refrigerator Systems
Micro-manipulated Probe Stations
LHe/LN₂ Cryostats
Magnet Systems

sales@janis.com www.janis.com
Click to view our product web page.

Deassociate the initial temporal phase deviation provided by photoelastic modulator for stroboscopic illumination polarization modulated ellipsometry

Hsiu-Ming Tsai, Chih-Wei Chen, Tsung-Han Tsai, and Yu-Faye Chao^{a)}

Department of Photonics and Institute of Electro-Optical Engineering, National Chiao Tung University, 1001 University Road, Tin ka-ping Photonics Center, Hsinchu 30010, Taiwan

(Received 30 November 2010; accepted 27 February 2011; published online 24 March 2011)

In addition to operating the imaging ellipsometric measurements by four-specific temporal phases in the photoelastic modulated ellipsometry, we added the fifth one to solve the initial phase of the photoelastic modulator. This methodology has been developed to conquer the slow imaging processing of charge-coupled device camera for the stroboscopic illumination in the polarization modulated imaging ellipsometry. Without any calibration in its initial phase, we can perform the ellipsometric measurement by the measurements of intensity at five-specific temporal phases. The intensities of a full cycle for a point on SiO₂/Si thin film were measured and analyzed for verifying this algorithm. The five stroboscopic illuminations were performed to measure the two-dimensional distribution of the same SiO₂/Si thin film. © 2011 American Institute of Physics. [doi:10.1063/1.3568745]

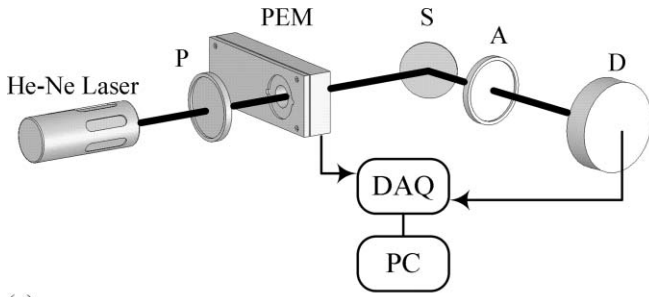
I. INTRODUCTION

Ellipsometry is a versatile tool for thin film measurements because it provides a nondestructive method to accurately determine the film thickness and optical constants.¹ Recently, imaging ellipsometry has been realized by using charge-coupled device (CCD) to carry out the ellipsometric measurement on surface instead of single point. Jin *et al.*² utilized the off-null concept to construct the imaging ellipsometer at pseudo-Brewster angle and obtained a 0.5 nm normal as well as 5 μm lateral resolution. But, its reliability in thickness measurement crucially depends on the chosen reference. Using CCD, Beaglehole³ combined the traditional rotating quarter-wave plate ellipsometry in measuring the surface thickness of a thin film through a 64 frames measurement in one cycle. In 2006, Chao *et al.*⁴ developed an analytical algorithm to obtain a set of ellipsometric parameters (EPs) by six intensity measurements in one cycle for a polarizer-sample-analyzer (PSA) ellipsometry, both parameters can be determined without any calibration in the azimuth positions of polarizer and analyzer. Then, they utilized this algorithm to obtain the surface thickness profile of a curved surface by employing six frames in a cycle in a simple PSA (Ref. 5) ellipsometry. However, the mechanical rotating element in ellipsometry can limit its speed in measuring EPs.

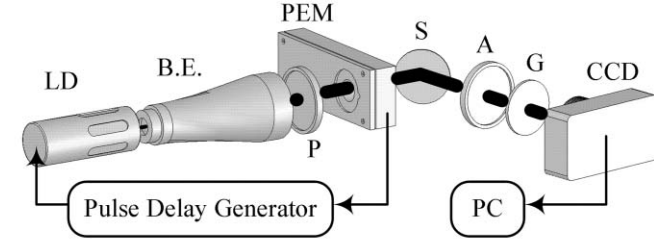
Since 1969,⁶ a modulator has been established to substitute the rotation component in ellipsometry for increasing the speed⁷ of measurements, such as acoustic-optical modulator, electro-optical modulator, spatial modulator, photoelastic modulator (PEM), etc. However, in this phase modulated ellipsometry, the imaging ellipsometry does face a new challenge: The data transfer rate of CCD is too slow to cope with the modulation frequency of a modulator. Povel *et al.*⁸

designed a mask to overcome the data transfer speed between these two devices. In 2006, Han and Chao⁹ presented a stroboscopic illumination technique to conquer the incompatibility between the fast modulation of PEM and slow data transfer of CCD by using the short laser pulses to freeze the intensity variation in PEM. This stroboscopic illumination technique provides four specific polarization states for polarization measurements, such as two-dimensional (2D) ellipsometric measurement. In addition, these four specific temporal polarization states have been proved¹⁰ to be the optimal choice for the stroboscopic illumination imaging polarimetry. Since the polarization state has to be frozen at the exact moment under the proper setups of modulation amplitude and azimuth position of optic axis of PEM, one has to calibrate the PEM system carefully. Chao¹¹ proposed an intensity ratio method to align the optical components in the photoelastic modulated polarimetry. According to Wang's^{12,13} proposition, one can calibrate the modulation amplitude of PEM for various wavelengths. For performing photoelastic modulated imaging ellipsometry, Han and Chao⁹ and Diner^{14,15} have noticed that the initial phase of optical signal of PEM is not synchronized with its reference signal. Han and Chao⁹ employed a reference sample to determine the intrinsic phase difference between the reference signal of PEM controller and the optical signal. In this paper, we propose to add the fifth polarization state for *in situ* deducing the intrinsic temporal phase delay of PEM. For verifying the ability of the method, we recorded the digitized waveform of a single spot measurement on SiO₂/Si thin film, then analyzed it by purposely shifting the zero position of initial temporal phase. In this work, we have proved that both the EPs and the initial phase can be obtained by these five polarization states. In the end, the two-dimensional thickness profile of the same sample has been used to demonstrate these five stroboscopic illumination technique, which proves that this method can deassociate its initial phase from the measurement of its EPs.

^{a)} Author to whom correspondence should be addressed. Electronic mail: yfchao@mail.nctu.edu.tw. Tel./fax.: +886-3-5731914.



(a)



(b)

FIG. 1. (a) Optical configuration for point measurement in photoelastic modulated ellipsometry. P, A: polarizer. PEM: photoelastic modulator. S: sample, D: photodetector, DAQ: data acquisition, PC: personal computer; (b) optical configuration of the stroboscopic illumination photoelastic modulated ellipsometry. LD: laser diode, B.E.: beam expander, G: ground glass, CCD: charge-coupled device.

II. THEORY

Ellipsometry measures the changes of polarization in the light which is reflected from the sample surface, this change can be used to deduce the optical parameters of sample. The EPs, ψ , and Δ , are defined as¹

$$\tan \psi e^{i\Delta} = \frac{r_p}{r_s}, \quad (1)$$

where r_p and r_s are the complex Fresnel reflection coefficients for the polarized light parallel and perpendicular to the plane of incidence, respectively. Substituting the compensator by a PEM in the polarizer–compensator–sample–analyzer setup, one can construct a photoelastic modulated ellipsometry to increase the speed of measurement and avoid the parasitic errors from the rotating components in the system. The data of this photoelastic modulated ellipsometry are acquired by a DAQ system, as shown in Fig. 1.

The Mueller matrices of PEM is expressed as

$$M_{\text{PEM}}(\Delta_P) = \begin{pmatrix} 1 & 0 & 0 & 0 \\ 0 & 1 & 0 & 0 \\ 0 & 0 & \cos \Delta_P & -\sin \Delta_P \\ 0 & 0 & \sin \Delta_P & \cos \Delta_P \end{pmatrix}, \quad (2)$$

where Δ_P is modulated as

$$\Delta_P = 2\pi \Delta_o \sin(\omega t), \quad (3)$$

with modulation amplitude, Δ_o . The Mueller matrix M_S of an

isotropic specimen¹ can be written as

$$M_S(\psi, \Delta) = \begin{pmatrix} 1 & -\cos(2\psi) & 0 & 0 \\ -\cos(2\psi) & 1 & 0 & 0 \\ 0 & 0 & \sin 2\psi \cos \Delta & \sin 2\psi \sin \Delta \\ 0 & 0 & -\sin 2\psi \sin \Delta & \sin 2\psi \cos \Delta \end{pmatrix}. \quad (4)$$

The final polarization state can be expressed as

$$S_f = M_A(A)M_S(\psi, \Delta)M_{\text{PEM}}(\Delta_P)S_p, \quad (5)$$

where the Stokes vectors S_f and S_p are the final polarization state and the incident light which is the linearly polarized light at the azimuth angle of P . The Mueller matrix of analyzer is

$$M_A(A) = \begin{pmatrix} 1 & \cos 2A & \sin 2A & 0 \\ \cos 2A & \cos^2 2A & \cos 2A \sin 2A & 0 \\ \sin 2A & \cos 2A \sin 2A & \sin^2 2A & 0 \\ 0 & 0 & 0 & 0 \end{pmatrix}, \quad (6)$$

while its transmission axis is at A . If the optic axis of PEM is at zero with respect to the incident plane, $P = -45^\circ$ and $A = 45^\circ$, the reflected intensity can be proved to be

$$I(\omega t) = \frac{I_o}{2}[1 - \sin 2\psi \cos(\Delta - \Delta_P)], \quad (7)$$

where I_o is the normalized intensity of the system. If the modulation amplitude (Δ_o) is 0.5, one can formulate the temporal intensity as

$$I(\omega t) = \frac{I_o}{2}[1 - \sin 2\psi \cos(\Delta - \pi \sin \omega t)]. \quad (8)$$

The EPs can be obtained by the following four specific polarization states: $\omega t = [0^\circ, 30^\circ, 90^\circ, \text{ and } 210^\circ]$,⁹ where ωt indicates the temporal phases. From Eq. (8), one can obtain the EPs through the following relations:

$$\begin{aligned} \sin 2\psi \cos \Delta &= \frac{I(90^\circ) - I(0^\circ)}{I(90^\circ) + I(0^\circ)}, \\ \sin 2\psi \sin \Delta &= \frac{I(210^\circ) - I(30^\circ)}{I(210^\circ) + I(30^\circ)}. \end{aligned} \quad (9)$$

It is worth to notice that these four polarization states are two pairs of orthogonal states in linear and circular.

The initial phase was calibrated by referring to a well calibrated sample⁹ for triggering the exact polarization state in stroboscopic illumination ellipsometry. This type of *ex situ* calibration may cause some unexpected system errors due to the exchange process of samples. Here, we assume that x is the shifted phase in its initial phase instead of predetermining it by a sample, then the temporal distribution of intensity $I'(\omega t)$ can be modified as

$$I'(\omega t) = \frac{1}{2}I_o\{1 - \sin 2\psi \cos[\Delta - \pi \sin(\omega t + x)]\}. \quad (10)$$

This system variable, x , can be solved by adding an extra temporal phase at $\omega t = 180^\circ$. From Eq. (10), one can prove

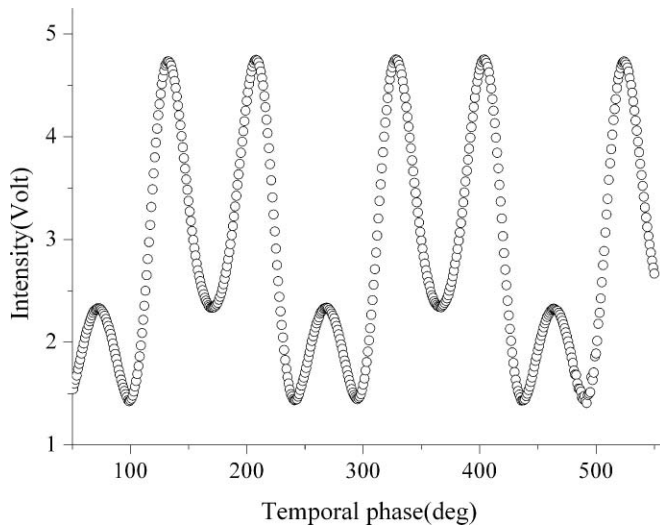


FIG. 2. Digitized waveform: typical DAQ temporal waveform of the measured SiO₂/Si thin film in PEM ellipsometry.

that

$$\frac{I'(210^\circ) - I'(30^\circ)}{I'(180^\circ) - I'(0^\circ)} = \frac{\sin[\pi \sin(x)]}{\sin[\pi \sin(x + \frac{\pi}{6})]}. \quad (11)$$

This ratio can eliminate the effect of EPs and normalized intensity, so it is free from the material under investigation. The shifted phase can be solved by the intensity measurements at 0°, 30°, 180°, and 210° according to Eq. (11). After solving the initial phase x , one can extract the value of Δ from the following:

$$\frac{I'(90^\circ) - I'(0^\circ)}{I'(210^\circ) - I'(30^\circ)} = \frac{-\sin\left[\frac{\pi[\cos(x) - \sin(x)]}{2}\right] \sin\left\{\Delta - \frac{\pi[\cos(x) + \sin(x)]}{2}\right\}}{\sin(\Delta) \sin\left[\pi \sin\left(x + \frac{\pi}{6}\right)\right]}. \quad (12)$$

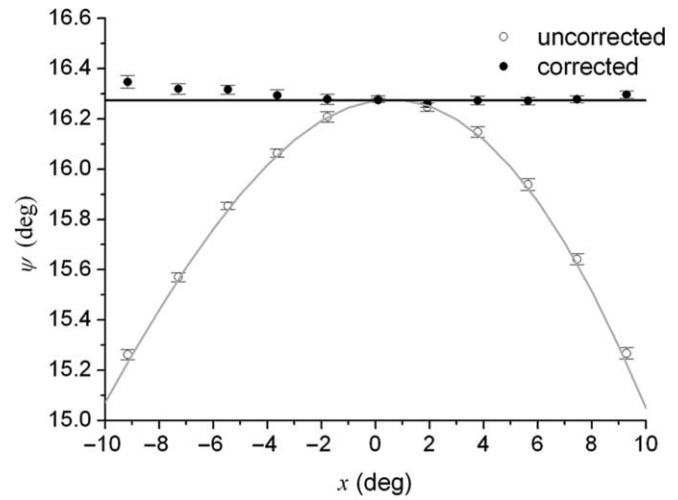
Again, one can easily obtain the value of ψ by substituting the obtained Δ and x into

$$\frac{I'(90^\circ) - I'(0^\circ)}{I'(90^\circ) + I'(0^\circ)} = \frac{-\sin(2\psi) \sin\left\{\Delta - \frac{\pi[\sin(x) + \cos(x)]}{2}\right\} \sin\left\{\frac{\pi[\sin(x) - \cos(x)]}{2}\right\}}{1 - \sin(2\psi) \cos\left\{\Delta - \frac{\pi[\sin(x) + \cos(x)]}{2}\right\} \cos\left\{\frac{\pi[\sin(x) - \cos(x)]}{2}\right\}}. \quad (13)$$

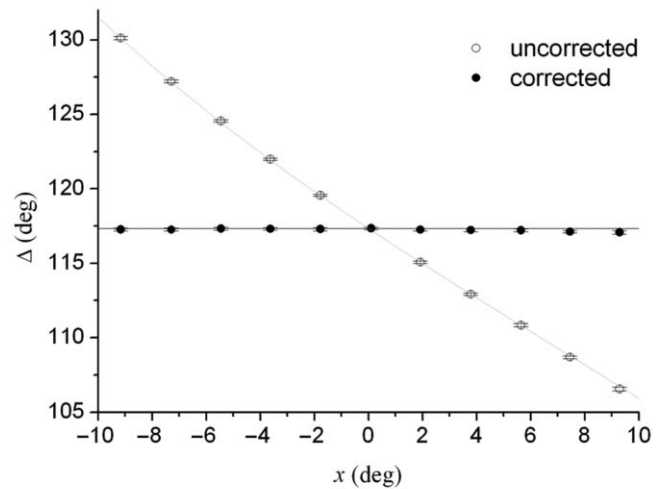
With the help of current symbolic mathematical program, one can avoid *ex situ* calibration errors completely through these complicated calculations.

III. SYSTEM CONFIGURATIONS

Two optical configurations for examining the methodology are shown in Figs. 1(a) and 1(b) by the measurement on a point and surface of the SiO₂/Si thin film, respectively. The ellipsometric system basically consisted of light source, polarizer, and PEM (PEM90/CF50, HINDS Instrument), while the reflected light from the sample went through an analyzer



(a)



(b)

FIG. 3. EPs vs the initial phase of PEM: Lines are the numerical simulated values under the purposely shifted x , (a) ψ , (b) Δ . Hollow gray and solid black circles are the uncorrected and corrected measured values, respectively. The corrected EPs for the SiO₂/Si thin film are $\psi = 16.27 \pm 0.02^\circ$ and $\Delta = 117.34 \pm 0.09^\circ$, respectively.

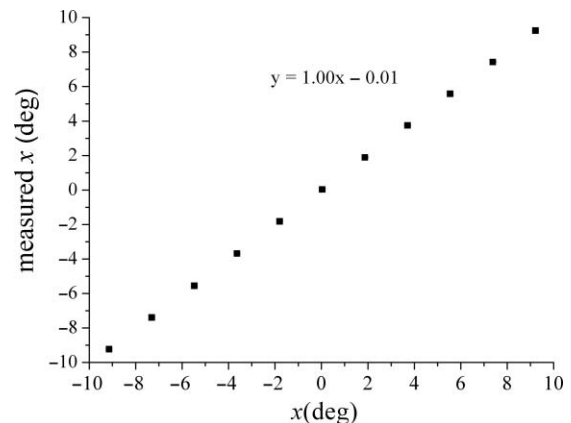


FIG. 4. The initial phase shift measured by the algorithm vs the purposely offset x from the waveform, which are averaged by ten cycles.

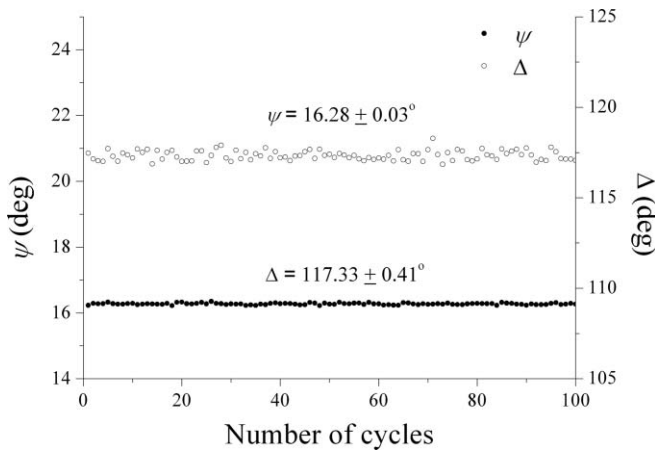


FIG. 5. Stability test of this method: The deduced Ψ and Δ were measured by the specific five polarization states in each cycle.

which was then recorded by a detecting system for parameters deduction. The transmission axis of polarizer and analyzer were fixed between -45° and 45° , respectively, and the optic axis of PEM was adjusted to be zero while its modulation amplitude was set at π for two wavelengths in this experiment. These entire azimuth angles of the system and modulation amplitude were well aligned and calibrated according to the Refs. 11–13. A CW laser (He–Ne laser, $\lambda = 632.8$ nm, 05-LHP-171, Melles Griot) was set at the incident angle of 70° to measure a point. The modulated intensities were received by an amplified photodetector (PDA55, Thorlabs). A DAQ system (PCI-6115, National Instrument) was used to record the 100 cycles for analyzing. For two-dimensional measurement around the same point of the SiO_2/Si thin film, we switched the CW laser to a pulse modulated laser diode (HITACHI, $\lambda = 658$ nm, HL6512MG) for performing stroboscopic illumination; its beam was expanded (Galilean beam expander, $\times 7$) and measured by a CCD camera (PIKE-032B) for imaging process. The modulated pulse was achieved by a dc bias current equal to the threshold value coupled with a programmable pulse generator (HP 8110A) to

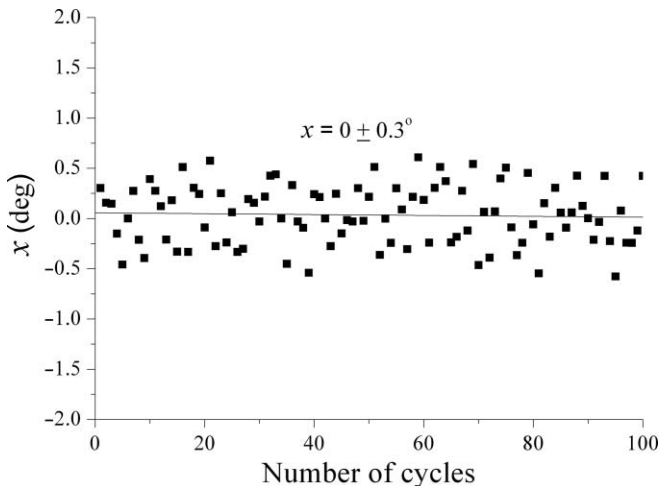


FIG. 6. The initial phases of PEM were measured by five polarization states in each cycle.

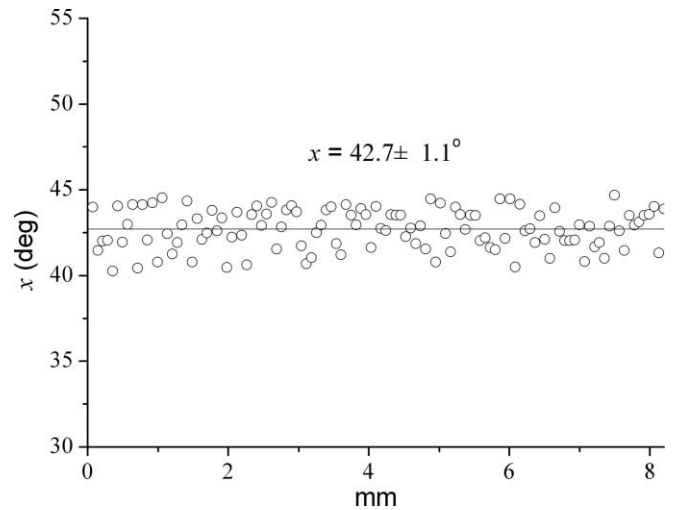


FIG. 7. The line profile is the initial phase value of the reference square wave, which was provided by Hinds PEM90.

drive the laser diode. A reference square wave provided by the PEM can be used to trigger the five specific temporal phases for the stroboscopic illumination pulse with a width of 108 ns ($\sim 2^\circ$ phase change of modulator). The exposure time of the CCD camera (640×480 pixels with a 16 bit gray scale) was set to be 80 ms for maintaining enough intensity in its linear range.⁹

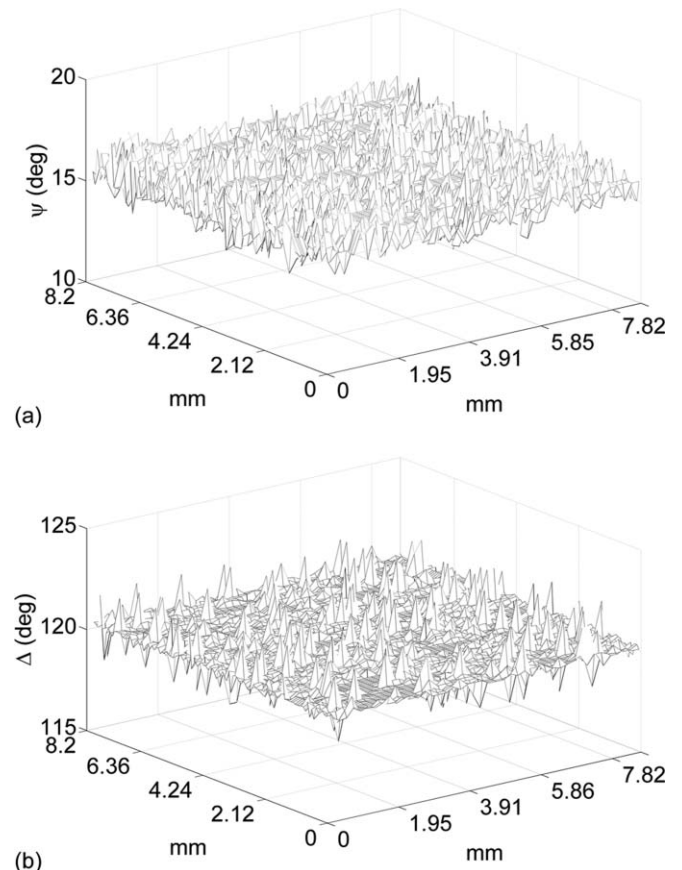


FIG. 8. Two-dimensional distribution of EPs of the SiO_2/Si thin film: (a) $\psi = 15.69 \pm 0.60^\circ$; (b) $\Delta = 120.16 \pm 0.35^\circ$.

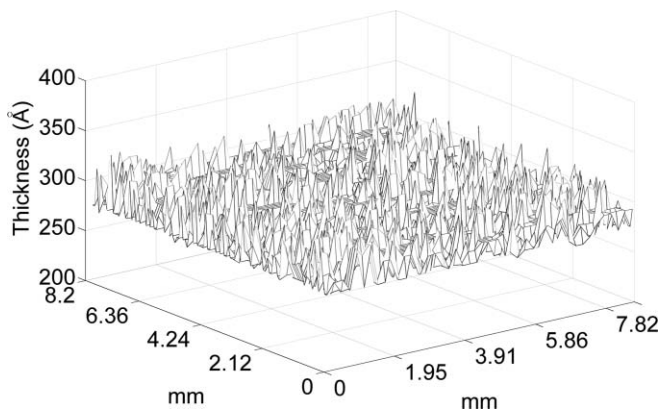


FIG. 9. The thickness distribution of the SiO_2/Si thin film: $d = 286 \pm 13 \text{ \AA}$.

IV. EXPERIMENTAL RESULTS

Using only five specific points in one cycle of the photoelastic modulated ellipsometry, we can prove that this method can be employed in the stroboscopic illumination ellipsometry. The 10 M sampling rate of DAQ system allows us to obtain the two adjacent temporal phases to be separated by 1.84° , as shown in Fig. 2. By averaging every ten cycles at those five specific phases, we extract the values of EPs and initial phase for verifying this method. Since we have recorded the full cycle, the initial phase can be offset artificially and then retrieve it to prove this technique. In addition to I_o , the physical parameters, x , ψ , and Δ can all be evaluated by these five specific phases.

For comparison, we simulated the deviations of ψ and Δ under the purposely shifted x , the simulated and experimental values for both parameters are compared before considering the shifted x to obtain the EPs through the Eq. (9) with respect to those results after substituting the value of x from Eq. (11) into Eqs. (12) and (13) to obtain the EPs, as shown in Figs. 3(a) and 3(b). Figure 3 clearly verifies that the system errors caused by the deviation of temporal phase can be corrected; this provides us enough confidence to extend this method in the 2D measurement. The values between the measured x versus the purposely offset x are only deviated by 1%, as shown in Fig. 4. The thickness of the oxidized silicon surface deduced from the measured EPs is 287 \AA . For substantiating the stability of this approach, we also obtained the EPs and the averaged initial phase x from the recorded digitized 100 cycles, as shown in Figs. 5 and 6. By comparing the simulated and measured values, one can observe the ability of this technique: the initial phase of PEM can be separately solved. Furthermore, in order to illustrate the method in two-dimensional measurement, we obtained the two-dimensional intensities of those five phases instead of preadjusting the intrinsic temporal phase of PEM. The intrinsic initial phase can be evaluated from Eq. (11). We only display a line profile for its initial phase to demonstrate the stability, as shown in

Fig. 7. After calculating the phase delay of the PEM, we then obtained the 2D EPs through Eqs. (12) and (13), as shown in Fig. 8. The thickness profile of the sample in 658 nm is $286 \pm 13 \text{ \AA}$, which is comparable to that measured on the single point, as shown in Fig. 9.

V. DISCUSSION AND CONCLUSION

The accuracy and precision in determining the physical properties of thin film depend on the measurements of EPs in ellipsometry. Applying our approach in PEM ellipsometry, we can independently solve the initial phase provided by the PEM controller without disturbing the measurements of EPs in imaging ellipsometry. On adding an additional temporal phase (i.e., 180°), this approach can also increase the accuracy of ellipsometric measurement. Thus, even the number for parameters extraction is drastically reduced in this technique, the measurements of EPs can still maintain its precision. Since there are no moving parts in stroboscopic illumination photoelastic modulated ellipsometry, this system not only avoids the parasitic error due to rotation, but it also breaks the time limit of mechanical rotation. Furthermore, the noise caused by the intensity fluctuation of laser can be reduced effectively because of the common path setup. Instead of using the overdetermination technique for Fourier transformation¹⁶ and least square methods¹⁷ to extract physical parameters in photoelastic modulated ellipsometry/polarimetry, we have provided a technique which performs the ellipsometric measurement by a limited number of measurements, so the imaging ellipsometry becomes feasible in a modulated system. Conclusively, this novel stroboscopic illumination ellipsometry, in conjunction with this methodology, ensures the accurate measurement in two-dimensional EPs.

¹R. M. A. Azzam and N. M. Bashara, *Ellipsometry and Polarized Light* (North-Holland, New York, 1989).

²G. Jin, R. Jansson, and H. Arwin, *Rev. Sci. Instrum.* **67**, 2930 (1996).

³D. Beaglehole, *Rev. Sci. Instrum.* **59**, 2557 (1988).

⁴Y. F. Chao, K. Y. Lee, and Y. D. Lin, *Appl. Opt.* **45**, 3935 (2006).

⁵C. Y. Han, Z. Y. Lee, and Y. F. Chao, *Appl. Opt.* **48**, 3139 (2009).

⁶J. C. Kemp, *J. Opt. Soc. Am.* **59**, 950 (1969).

⁷D. B. Chenault and R. A. Chipman, *Appl. Opt.* **32**, 3513 (1993).

⁸H. Povel, H. Aebbersold, and J. O. Stenflo, *Appl. Opt.* **29**, 1186 (1990).

⁹Y. F. Chao and C. Y. Han, *Rev. Sci. Instrum.* **77**, 032107 1 (2007).

¹⁰H. M. Tsai and Y. F. Chao, *Opt. Lett.* **34**, 2279 (2009).

¹¹Y. F. Chao, *SPIE* **4833**, 317 (2003).

¹²M. W. Wang, Y. F. Chao, K. C. Leou, F. H. Tsai, T. L. Lin, S. S. Chen, and Y. W. Liu, *Jpn. J. Appl. Phys.* **43**, 827 (2004).

¹³M. W. Wang, F. H. Tsai, and Y. F. Chao, *Thin Solid Films* **455–456**, 78 (2004).

¹⁴D. J. Diner, A. Davis, B. Hancock, G. Gutt, R. A. Chipman, and B. Cairns, *Appl. Opt.* **46**, 8428 (2007).

¹⁵D. J. Diner, A. Davis, B. Hancock, S. Geier, B. Rheingans, V. Jovanovic, M. Bull, D. M. Rider, R. A. Chipman, A. B. Mahler, and S. C. McClain, *Appl. Opt.* **49**, 2929 (2010).

¹⁶E. Meyer, H. Frede, and H. Knof, *J. Appl. Phys.* **38**, 3682 (1967).

¹⁷D. E. Aspnes, *Opt. Commun.* **8**, 222 (1973).